科学通报 2017 年 第 62 卷 第 6 期：508 ~ 518
专辑：胶体与界面化学 进 展
《中国科学》杂志社
SCIENCE CHINA PRESS

基于单层胶体晶体的功能性二维有序阵列研究进展

李扬，王文慧，齐利民*

北京大学化学与分子工程学院，北京分子科学国家实验室，北京 100871
* 联系人，E-mail: liminqi@pku.edu.cn

2016-07-27 收稿，2016-08-10 修回，2016-08-12 接受，2016-09-13 网络版发表
国家重大科学研究计划(2013CB932601)和国家自然科学基金(21473004)资助

摘要 二维有序微纳米结构阵列往往呈现出有序图案化结构所带来的新颖或增强的性质，由胶体球自组装而成的单层胶体晶体已被广泛应用于二维有序微纳米结构阵列的可控制备. 这种方法具有简单、高效、适用范围广等诸多优点，因而愈来愈受到人们的关注. 本文简要综述了近年来基于单层胶体晶体的功能性二维有序阵列的研究进展，主要包括二维光子晶体传感器、等离激元纳米阵列、太阳能转换器件、光学与光电器件、表面浸润与黏附以及生物医学材料等方面的最新成果. 其中着重介绍了本课题组在ZnS纳米碗阵列、异质结构Ag_2S-Ag纳米碗阵列、异质结构TiO_2纳米棒@纳米碗阵列以及方解石单晶微透镜阵列等方面所取得的一些研究进展.

关键词 单层胶体晶体，胶体球刻蚀法，二维有序阵列，纳米结构，微结构

二维有序微纳米结构阵列往往呈现出有序图案化结构所带来的新颖或增强的性质，在二维光子晶体、光学与光电器件、能源转换与存储、生物和化学传感、分离与控释、表面浸润与黏附、生物组织工程、减反射涂层以及超材料等诸多领域有着广阔的应用前景[1~6]. 因此，人们一直致力于发展可高效制备结构参数可调的大面积二维有序微纳米结构阵列的表面图案化技术. 相比于传统的刻蚀技术(如光刻、电子束刻蚀、X-射线刻蚀等)和新兴的纳米压印、沾笔刻蚀、微接触印刷等技术，基于胶体自组装结构的表面微纳米图案化技术因其低成本、低耗时、高产量等特点而引起人们的极大兴趣[7,8]. 作为一种典型的二维结构化的胶体自组装结构，单层胶体晶体(MCC)被广泛用于各类二维有序微纳米阵列的可控制备. 这种以单层胶体晶体作为模板进行沉积或蚀刻的二维图案化技术通常被称作为胶体球刻蚀法(或纳米球刻蚀法, NSL)，它具有简单、廉价、高效、适用范围广以及结构参数易于调变等优点，因而日益受到人们的重视[9~13]. 作为二维模板的单层胶体晶体可以附着于固体表面进行气固或液固界面上沉积、生长和蚀刻，从而得到具有二维有序阵列结构的固体表面；另一方面，单层胶体晶体可以漂浮于液体表面进行气液界面沉积，从而得到漂浮于液体表面的由二维有序阵列构成的自支撑多孔薄膜[14]. 随着胶体球刻蚀技术的不断发展和完善，近年来人们致力于利用该技术获得一些具有特殊功能或优异性能的功能性二维有序微纳米结构阵列，并取得了不少突出成果. 本文将简要综述该领域的最新进展情况，并着重介绍本课题组近期在该领域取得的一些研究结果.

1 二维光子晶体传感器

二维有序微纳米结构阵列由于具有周期性变化的介电常数，因而存在对应于二维光子晶体的光子带隙. 光子带隙的位置与结构本身的晶格参数及周围环境的介电常数(或折光指数)有直接关联，因而可以通过外部环境所变化引起的晶格间距或有效折光

引用格式: 李扬，王文慧，齐利民. 基于单层胶体晶体的功能性二维有序阵列研究进展. 科学通报, 2017, 62: 508–518
Li Y, Wang W H, Qi L M. Progress in functional 2D ordered arrays based on monolayer colloidal crystals (in Chinese). Chin Sci Bull, 2017, 62: 508–518, doi: 10.1360/N972016-00824

指数的变化来实现传感或检测功能. 单层胶体晶体及其二维反复制结构均构成典型的二维光子晶体, 在适当条件下可以发挥二维光子晶体传感器的作用[15].

本课题组[9]曾利用基于气体扩散反应的气液界面胶体球刻蚀法实现了多种无机纳米网和纳米碗阵列的可控制备. ZnS是一种高折射率(n~2.35)的宽带隙半导体材料, 在构筑基于可见及近红外光的二维光子晶体方面具有独特的优势. 本课题组[16]采用基于直接液相沉积的气液界面胶体球刻蚀法成功制备了大面积规整有序的ZnS纳米碗阵列. 将聚苯乙烯(PS)胶球组装而成的MCC转移至包含有醋酸锌、硫代乙酰胺(TAA)、乙二胺四乙酸二钠(Na_2EDTA)和醋酸铵的混合溶液表面, 利用TAA在溶液中逐渐释放出的S^{2-}与Zn^{2+}发生反应, 即可在胶球的底部原位生成ZnS纳米碗, 在将PS胶球溶解去除之后即可制得到ZnS纳米碗阵列薄膜(图1(a)). 若以600 nm的胶球为模板, 则可得到晶格间距约为600 nm、壁厚约为80 nm的规整有序的ZnS纳米碗阵列(图1(b)和(c)). ZnS纳米碗阵列的二维光子带隙与周围介质的折光指数密切相关, 因此构成一类对于环境折光指数具有灵敏响应性的二维光子晶体传感器, 可用于有机溶剂的可视化检测和生物分子的灵敏检测. 图1(d)给出了浸泡于不同有机溶剂中的ZnS纳米碗阵列的透射光谱. 随着空气、乙醇、甲苯的折光指数的依次增大, 透射波谷发生明显的红移. 其透射波谷或光子带隙与溶剂的折光指数之间存在良好的线性关系(图1(e)), 检测灵敏度高达266 nm/RIU. 若将其浸泡在乙醇、十六烷、甲苯中时, 它的颜色相应地变为蓝色、黄色与红色. 因此, 该ZnS纳米碗阵列可以被用作灵敏度高、快

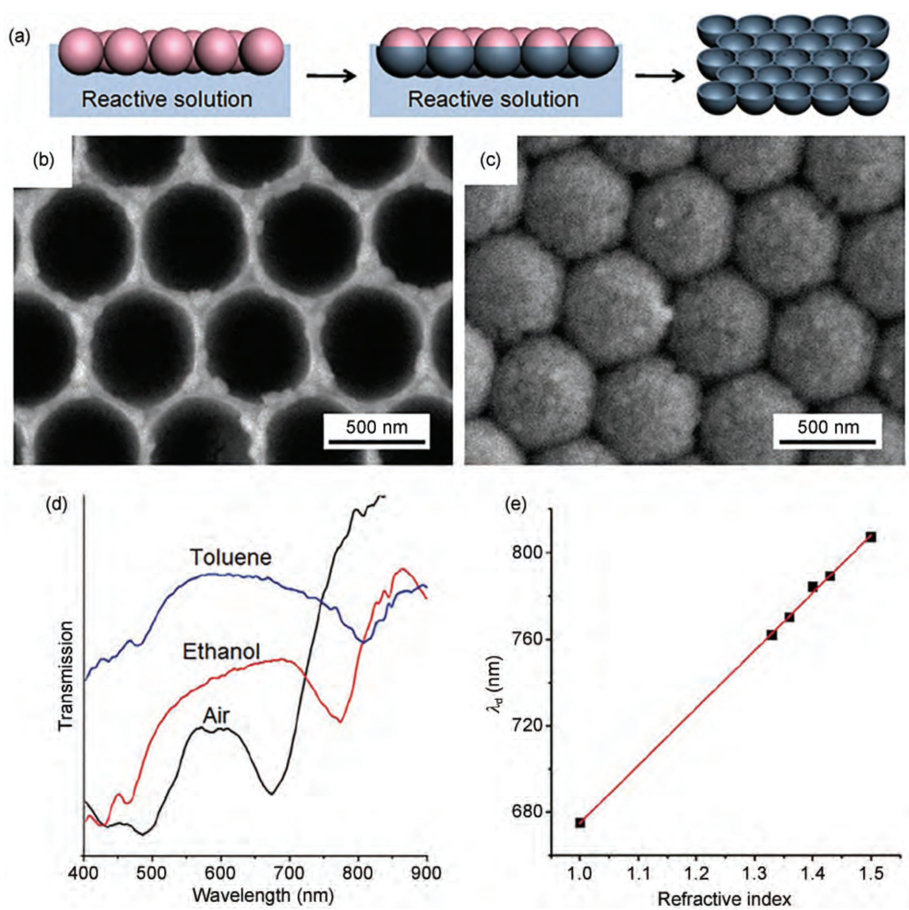

图 1 (网络版彩色)(a) 基于液相沉积的气液界面胶体球刻蚀法制备纳米碗阵列示意图; ZnS纳米碗阵列的正面(b)和背面(c)扫描电子显微镜(SEM)照片; (d) 不同溶剂中ZnS纳米碗阵列的透射光谱; (e) 透射波谷随溶剂折光指数的变化[16]

Figure 1 (Color online) (a) Schematic illustration of the fabrication of nanobowl arrays by nanosphere lithography at the gas-liquid interface via solution deposition. Top-view (b) and bottom-view (c) SEM images of ZnS nanobowl arrays. (d) Transmission spectra of ZnS nanobowl arrays immersed in different organic solvents. (e) Relationship between the stop band position and the refractive index of solvents[16]

速及可视化的二维光子晶体传感器. 此外, 若将生物素标记的牛血清白蛋白修饰到ZnS纳米碗阵列基底上, 结合生物素与抗生物素蛋白的特异性识别, 还可实现对抗生物素蛋白的快速定量检测. 除了具有低检出限和宽检测范围(100 pmol/L~100 nmol/L)的特点外, 该阵列的开放式碗状结构有利于待检测分子的快速吸附.

李澄课题组[17]通过将MCC浸入反应液中原位晶化的方法制备了表面包裹了金属有机框架化合物(MOF)超薄层的单层胶体晶体, 借助于MOF材料独特的气体吸附性能, 制备了具有高灵敏气体传感性能的二维光子晶体传感器. 最近, 他们利用气液界面胶体球刻蚀法成功制备了大面积规整有序的、具有不对称结构的MOF纳米碗阵列薄膜[18]. 该纳米碗阵列所具有的二维光子晶体特性和多级孔结构使其同时具有气体传感、纳米粒子筛分和染料分子吸附等多重功能.

如果将单层胶体晶体直接包埋在具有环境响应特性的水凝胶介质中, 则可以制备出基于晶格间距变化的二维光子晶体传感器. Asher课题组[15]在这方面开展了系统的研究工作, 最近他们[19]根据这一原理成功制备出了对白念珠菌具有灵敏响应性的蛋白质水凝胶二维光子晶体传感器. 将非密堆积的单层胶体晶体包埋在伴刀豆球蛋白水凝胶中构成一个体积可以变化的二维光子晶体, 这种蛋白质可以选择性地与白念珠菌细胞表面的甘露聚糖进行多配位键合, 导致蛋白质水凝胶的收缩和晶格间距的缩小, 进而造成衍射光的蓝移. 该结果为通过特异识别作用在水溶液环境中检测微生物开辟了一条新的途径. 由普通聚合物胶球构成的单层胶体晶体的折光指数通常较低, 因而其衍射光的强度受到一定的限制. 针对这一问题, 李越课题组[20]最近制备了一种由二维有序的Au纳米球阵列附着于水凝胶表面所构成的二维光子晶体传感器, 它呈现出超高的衍射光强度, 在可视化检测领域具有潜在的应用价值.

2 等离激元纳米阵列

一些金属(如金、银等)存在显著的表面等离激元共振(SPR)效应, 其二维有序纳米结构阵列也被称作为等离激元纳米阵列. 这种具有独特SPR性质的等离激元纳米阵列结构在表面增强拉曼散射(SERS)、基于SPR效应的分子检测、纳米光学、光捕获以及超材料等领域具有广阔的应用前景[21]. 基于MCC模板的胶体球刻蚀法则为等离激元纳米阵列的可控制备提供了一条行之有效的便捷途径.

本课题组[22]曾通过气液界面胶体球刻蚀法制备出大面积规整有序的金属Ag纳米碗阵列. 这种具有较高机械强度的二维有序大孔金属薄膜呈现出鲜艳的表观颜色, 是一类典型的等离激元纳米阵列结构. 由于具有周期性的表面尖端结构, 它可以作为具有较高增强因子的SERS基底; 另一方面, 由于其SPR共振峰呈现出显著的环境响应性, 它还可作为SPR传感器用于生物大分子的灵敏检测. 由于胶体球刻蚀法制备的二维有序金属纳米阵列兼具SERS和SPR检测功能, 这方面的研究一直受到人们的关注. 例如, Oh课题组[23]利用原子层沉积结合胶体球刻蚀法实现了具有10 nm环状间隙的SERS基底的可控制备. 他们以PS胶球构成的MCC为模板, 通过Ag, Al_2O_3, Ag的交替沉积和随后的选择性蚀刻, 得到了结构新颖的纳米圆环状Ag间缝隙的二维有序纳米阵列. 对于间隙为10 nm的等离激元纳米阵列, 在环状纳米间隙位置处拉曼散射的增强因子达到10^8, 因而该纳米阵列可以作为高度信号均一性的高灵敏SERS基底. 与此同时, 该等离激元纳米阵列的局域等离激元共振(LSPR)吸收峰的位置呈现出显著的环境依赖性, 可以作为有效的LSPR生物传感器.

近年来, 人们仍然致力于通过进一步发展胶体球刻蚀技术来设计制备出具有新颖或优化结构的等离激元纳米阵列, 以期获得可调的等离激元性质和优异的SERS性能, 同时发掘其在其他诸多领域中的潜在应用. 例如, Huang课题组[24]通过将MCC模板的掩膜作用和支架作用相结合, 并借助于后续热处理过程, 实现了具有多重周期的Au纳米粒子阵列的可控制备. 这种技术可以有效制备出具有二元和三元表面图案的等离激元纳米阵列结构, 将有助于获得可调的等离激元性质和优化的SERS性能. Huang课题组[25]还通过具有位点选择性的电化学生长法在PS构成的MCC模板的上半球表面上选择性沉积一层Ag薄膜, 得到具有超疏水性的PS-Ag双面粒子有序阵列. 这种超疏水性等离激元纳米阵列有利于待测分子在表面的富集, 从而实现对fmol/L量级稀溶液的高灵敏SERS检测. 蔡伟平课题组[26]在部分刻蚀后的MCC模板上进行金属沉积得到了新颖的Au纳米环-纳米壳二元结构. 与单纯的纳米壳结构相比, 二元结构阵列中

纳米环的引入带来SPR吸收强度的提高和SERS效果的增强. Jiang课题组[27]通过对两种胶体球构成的单层二元胶体晶体进行氧等离子体刻蚀，然后在不同刻蚀时间得到的胶体球模板上沉积金属Ag，得到了粒子形貌及间隙可调的Ag纳米粒子阵列，并可实现高灵敏的SERS检测. Wachsmann-Hogiu课题组[28]利用聚二甲基硅氧烷(PDMS)对刻蚀得到的非密堆MCC进行反复制，得到PDMS的纳米碗阵列，再在碗的内表面溅射沉积上40 nm厚的Ag层，即可得到有利于待测分子吸附和拉曼信号检测的Ag纳米碗阵列. 李越课题组[29]通过化学沉积与物理沉积相结合的方法制备出不同形貌的氧化铁纳米碗阵列，然后磁控溅射上Au的薄层，在优化条件下得到了具有高度稳定性的高灵敏SERS基底. 李越课题组[30]还采用类似的化学沉积与物理沉积相结合的方法制备了带有表面Au包覆层的球形纳米粒子的有序阵列，它具有可调节的粒子间纳米缝隙，在经过表面化学修饰之后还可以实现疏水性增强的快速SERS检测功能. 最近，Ghosh课题组[31]利用MCC模板制备出了由单层石墨烯分隔开的一对Ag纳米粒子的二维有序阵列，这种原子级分隔的等离激元双粒子呈现出超高的电磁场增强和光响应，在SERS和光电器件等领域有潜在的应用价值.

3 太阳能转换器件的光电极

光电化学分解水和太阳能电池是两类重要的太阳能转换技术，而光电化学池和太阳能电池中的光电极则是二者的核心组成部分，对于其光电转换性能有着非常重要的影响. 基于单层胶体晶体的二维有序微纳米结构阵列在各类光电极的制备和性能改善中发挥着积极作用.

以MCC为模板复制得到的二维有序纳米碗阵列结构可以造成入射光在碗内壁的多次散射，有利于促进光的捕获，从而在作为光电化学分解水的光阳极时获得显著增强的性能. 在之前利用气液界面胶体球刻蚀法制备了Ag_2S纳米网[32]和Ag纳米碗阵列[22]的基础上，本课题组[33]将气液界面胶体球刻蚀法拓展至二元复合纳米阵列结构的制备，通过两步气液界面胶体球刻蚀法实现了异质结构Ag_2S-Ag纳米碗阵列的可控制备. 以漂浮在$AgNO_3$溶液表面的MCC作为模板，在体系中先引入H_2S气体生成Ag_2S纳米网，再引入N_2H_4/NH_3混合气体生成附着于Ag_2S纳米网下面的Ag纳米碗阵列，从而制备得到大面积连续的Ag_2S-Ag异质结构纳米碗阵列(图2(a)). 若将转移至FTO基底上的Ag_2S-Ag异质结构纳米碗阵列作为光电化学池的光阳极，可以呈现出显著增强的光电化学分解水性能(图2(b)). 一方面Ag纳米碗层的存在有利于光生电子由Ag_2S向Pt电极的传递及由此带来的电荷分离，另一方面, Ag纳米碗有利于光线在其内部的多次散射，从而有利于光的捕获利用. 在外加偏压为1.23 V时，Ag_2S-Ag异质结构纳米碗阵列的光电流密度为17.9 μA/cm^2，较之单纯Ag_2S纳米网的光电流密度(2.1 μA/cm^2)有很大提高，表现出显著增强的光催化活性(图2(c)).

作为一种典型的光电化学分解水的光阳极材料，TiO_2因其优异的光催化性质、高的稳定性以及廉价无毒的特性而受到人们的广泛关注. 最近，本课题组[34]将二次生长与气液界面胶体球刻蚀法相结合，成功制备得到结构新颖的异质结构TiO_2纳米棒@纳米碗阵列. 首先利用气液界面胶体球刻蚀法制备得到TiO_2纳米碗(NB)阵列，然后通过简便的水热法在转移至FTO基底上的纳米碗的内壁生长出锐钛矿型TiO_2纳米棒(NR)阵列(图3(a)). 该异质结构纳米棒@纳米碗(NR@NB)阵列因具有多重散射中心而表现出优异的光捕获能力(图3(b)); 其高的表面积有利于TiO_2与电解质的接触，纳米棒的一维结构有利于电子的传输；此外，金红石/锐钛矿异质节的存在可进一步促进电荷分离. 该异质结构NR@NB阵列作为光阳极时呈现出显著增强的光电化学分解的能力，在外加偏压为1.23 V时光电流密度达到1.24 mA/cm^2，较之普通TiO_2纳米棒阵列的光电流密度(0.68 mA/cm^2)几乎增加了1倍(图3(c)). 值得一提的是，最近熊宇杰课题组[35]通过将Au纳米粒子限制在氮掺杂TiO_2纳米碗阵列的内表面，借助于Au纳米粒子的等离激元增强效应实现了全光谱范围光解水性能的显著提高.

以MCC为模板制备的纳米阵列结构在光电化学分解水的光阴极方面也能够发挥重要作用. 例如，通过胶体球刻蚀法制备的Ti/Pt纳米网结构作为催化剂可以显著提高Si基光阴极在光电化学还原水过程中的光电转换效率[36]. 该纳米网的结构参数对于其催化效果有着显著的影响.

二维有序的图案化纳米阵列往往具有显著的减反射性能[5]，可以增强对光的捕获能力，因此在硅基薄膜太阳能电池中有着广泛的应用. 例如，利用胶体

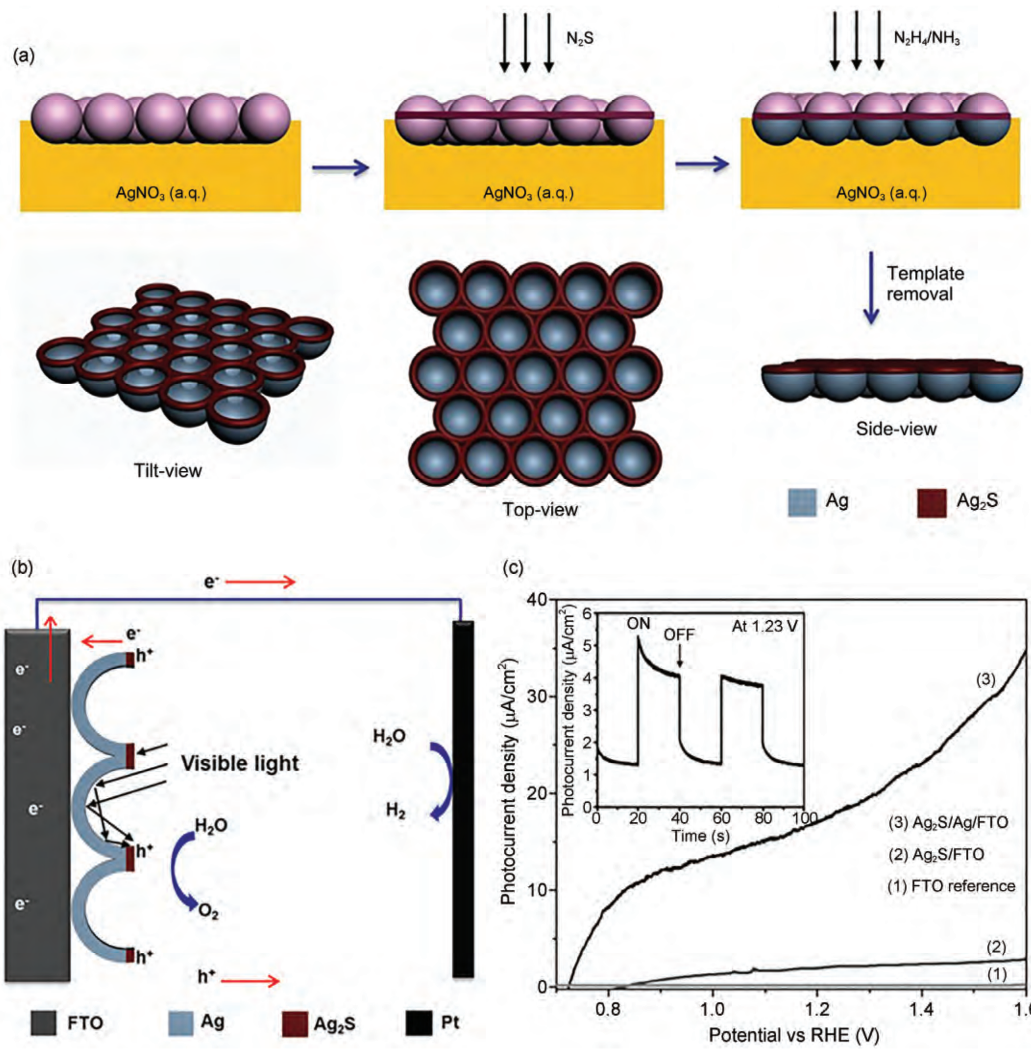

图 2 (网络版彩色)(a) 两步气液界面胶体球刻蚀法制备异质结构Ag_2S-Ag纳米碗阵列的示意图; (b) 以Ag_2S/Ag/FTO为光阳极的光电化学池工作原理图; (c) 可见光照射下不同光阳极的光电流密度曲线[33]

Figure 2 (Color online) (a) Schematic illustration of the fabrication of Ag_2S-Ag heterostructured nanobowl arrays by two-step nanosphere lithography at the gas-liquid interface. (b) Schematic diagram of electron/hole transport for water splitting in an Ag_2S/Ag/FTO photoelectrochemcial cell using the Ag/Ag_2S/FTO as the photoanode. (c) Linear sweep voltammograms curves under visible light illumination[33]

球刻蚀法制备的Si半球有序阵列呈现出显著的减反射性能，相应的硅基太阳能电池的光电转换效率达到5.9%，较之平面Si结构有了25%的提高[37]．另一方面，空心球壳的单层有序阵列通常具有较高的表面积且有利于电解质的注入，并且具有增强的光散射能力，因而可被用于染料敏化太阳能电池领域．例如，由以MCC为模板制备的TiO_2空心半球壳有序阵列被应用于染料敏化太阳能电池的光阳极材料，在优化条件下获得了3.49%的光电转换效率[38]，但其相对较低的表面积和染料吸附量在很大程度上限制了其光电转换效率的进一步提升．值得一提的是，随着近期有机-无机杂化钙钛矿太阳能电池的迅速发展，胶体球刻蚀法也开始在钙钛矿太阳能电池中得到应用．例如，Snaith课题组[39]利用胶体球刻蚀法制备了钙钛矿纳米碗阵列，进而制备出了光电转换效率为9.5%的钙钛矿太阳能电池．此后，Chen课题组[40]通过制备大面积规整有序的钙钛矿纳米碗阵列，获得了具有二维光子晶体特性的彩色钙钛矿太阳能电池，其光电转换效率可达到11.2%．最近，杨世和课题组[41]将TiO_2纳米碗阵列作为钙钛矿太阳能电池的电子传输层，可以起到促进光吸收的作用，钙钛矿太阳能电池的性能因此得到优化，光电转换效率达到12.02%．

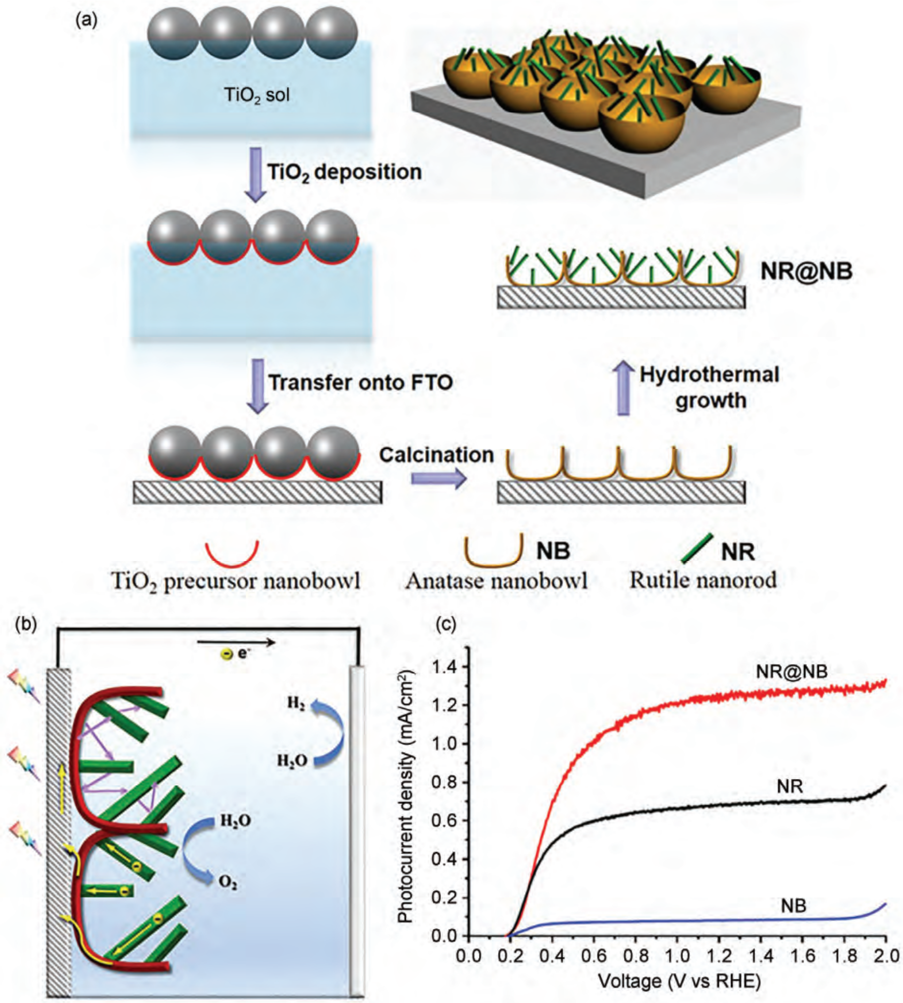

图 3 (网络版彩色)(a) 气液界面胶体球刻蚀结合二次生长法制备异质结构TiO_2 NR@NB阵列的示意图; (b) 以TiO_2 NR@NB阵列为光阳极的光电化学池工作原理图; (c) 模拟太阳光照射下不同光阳极的光电流密度曲线[34]

Figure 3 (Color online) (a) Schematic illustration of the preparation process of TiO_2 NR@NB arrays. (b) Schematic diagram of the light scattering and electron transport in TiO_2 NR@NB array electrode for photoelectrochemical water splitting. (c) Linear sweep voltammograms of TiO_2 NB, NR, and NR@NB array electrodes recorded in a 1 mol/L NaOH solution under simulated one sun illumination (AM 1.5G, 100 mW/cm^2)[34]

4 微透镜阵列

微透镜阵列(MLA)是指由孔径处于数微米至数百微米范围的微小透镜有序排列而成的二维阵列，在数码相机、光学通讯、三维成像以及人工复眼等领域有广阔的应用前景. 海蛇尾是一种著名的深海海洋生物，其中光敏感性海蛇尾的外骨骼由方解石单晶微透镜阵列构成，发挥着机械保护和感光的双重功能[42]. 受到海蛇尾微透镜阵列结构的启发，仿生制备单晶微透镜阵列成为多年来人们努力追求的一个目标. 本课题组[43]早期曾利用基于无定形前体转化的胶体晶体模板法制备了三维有序大孔方解石单晶；在此基础上，本课题组[44]利用气液界面胶体球刻蚀法制备了碳酸钙纳米碗阵列，但最终只能得到多晶形式的方解石纳米碗阵列，不能起到光学成像的作用.

最近，本课题组[45]采用单层胶体晶体模板辅助的外延生长法，首次实现了由方解石单晶构成的微透镜阵列的人工合成. 图4(a)为制备过程示意图，首先选取具有特定晶体取向的方解石单晶片，然后将MCC转移至其表面，经过一段时间的外延生长，去除模板之后即可得到由方解石单晶构成的微小凹透镜阵列. 通过选取具有(104)和(001)暴露面的方解石单晶片，即可分别得到(104)取向和(001)取向的方解

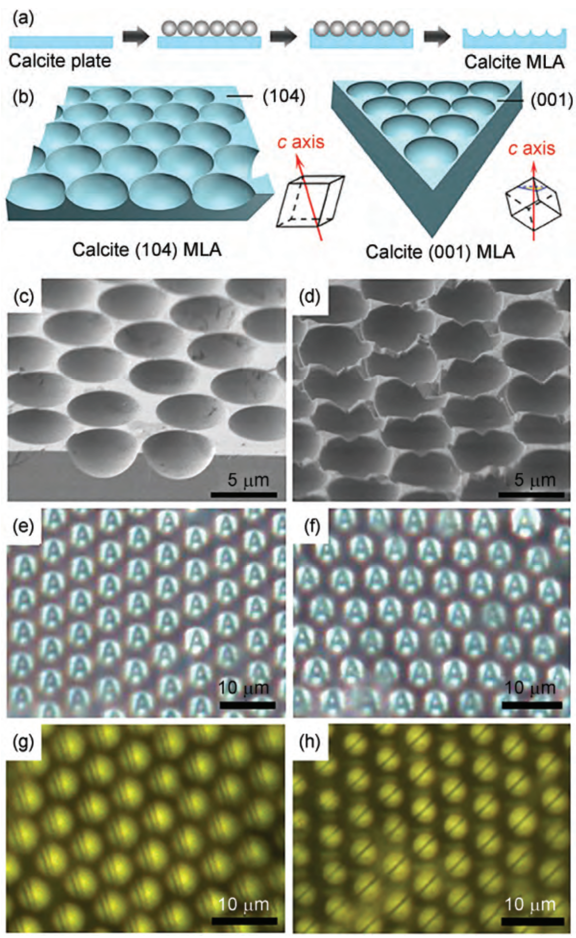

图 4 (网络版彩色)(a) 单层胶体晶体辅助外延生长法制备单晶方解石微透镜阵列(MLA)示意图; (b) (104)和(001)晶面取向的微透镜阵列结构示意图; (104)晶面取向(c)和(001)晶面取向(d)的微透镜阵列的SEM照片; (104)晶面取向(e, g)和(001)晶面取向(f, h)的微透镜阵列分别对字母A(e, f)和头发丝(g, h)成像的光学显微镜照片[45]

Figure 4 (Color online) (a) Schematic illustration of the fabrication of single crystal calcite microlens arrays (MLAs) through MCC-assisted, epitaxial growth on calcite plate. (b) Structure and crystal orientation of calcite (104) and (001) MLAs. The optical axis of rhombohedral calcite crystal is along the *c* axis indicated by the arrows. (c), (d) SEM images of calcite (104) and (001) MLAs, respectively. (e), (f) Optical microscopy (OM) images of "A" arrays projected by calcite (104) and (001) MLAs, respectively. (g), (h) OM images of hair arrays projected by calcite (104) and (001) MLAs, respectively[45]

石MLA(图4(b)), 其中方解石晶体的*c*轴方向即为该双折射晶体的光轴方向. 图4(c)和(d)分别给出了(104)取向和(001)取向的方解石MLA的SEM照片, 它们可以直接用于光学成像. 若以1 cm^2大小的字母"A"为成像对象, 则二者均可得到清晰的像(图4(e), (f)); 但如果以70 μm直径的细头发丝作为成像对象, (104)取向的MLA由于双折射而只能得到含有两条线的重影(图4(g)), (001)取向的MLA则能够有效避免双折射而形成单一清晰的像(图4(h)). 此外, 在正交偏振锥光系统下, 两种微透镜阵列均呈现出独特的偏振依赖光学性质. 该结果对于仿生制备单晶微结构阵列并探索其光学性质具有重要的借鉴意义.

5 其他功能性二维有序阵列

除了上述研究进展之外, 基于单层胶体晶体的二维有序微纳米结构阵列在其他一些功能材料体系中的应用也受到人们的关注. 李广涛课题组[46]制备了金薄膜表面的介电氧化物亚微米碗阵列并研究了其光学性质, 这种新型的光子晶体-表面等离激元杂化材料预期在传感等领域有着潜在应用价值. 若将单层有序排列的Au纳米海胆结构置于石英晶体微天平的传感器上, 可以制备出对Hg蒸气有灵敏响应的气体传感器[47]. 李越课题组[48]利用单层胶体晶体作为模板制备了Cu纳米粒子@石墨烯核壳型复合结构的大面积有序阵列, 它呈现出优异的催化性能. 武利民课题组[49]制备了高质量的$Ni_xMg_{1-x}O$纳米碗阵列, 发现它具有显著增强的光响应性能, 可望在光检测器方面有潜在的应用. 利用胶体球刻蚀法制备的Cu纳米网[50]和ITO纳米蜂窝结构[51]在作为光电器件重要构成单元的透明电极方面有广阔应用前景. Dev等人[52]利用界面能驱动的胶体球刻蚀技术在Si表面制备了ZnO纳米线簇集体的有序阵列, 使得Si表面的总反射率大大降低. 此外, 基于单层胶体晶体的球形透镜光刻技术(SLPL)可以制备结构可控的有序纳米结构阵列, 在发光二极管等领域有着广阔应用前景[13].

Aizenberg课题组[53]以单层胶体晶体为模板制备得到透明的纳米孔表面结构, 可作为一类具有一定机械强度的图案化疏液润滑表面. Chung课题组[54]通过对紫外光固化树脂包埋的单层胶体晶体进行溶剂处理制备了具有很高黏附力的纳米吸管阵列. Scherman课题组[55]则通过超分子作用辅助下的单层胶体晶体模板法实现了二元聚合物刷的亚微米和纳米图案化, 在具有双重响应的传感薄膜和生物医学涂层领域有着潜在应用价值. 此外, Kingshott课题组[56]将胶体球刻蚀法与掠射角沉积技术相结合制备了具有良好生物相容性的金属Ta的图案化纳米结构阵列, 可用于有效调制人类间充质干细胞的行为.

6 结语

由胶体球自组装而成的单层胶体晶体已被广泛

应用于二维有序微纳米结构阵列的可控制备. 这种方法具有简单、高效、适用范围广、结构参数易调变等诸多优点, 因而愈来愈受到人们的关注. 近期的研究工作表明, 基于单层胶体晶体的功能性二维有序阵列在二维光子晶体传感器、等离激元纳米阵列、太阳能转换器件、光学与光电器件、表面浸润与黏附以及生物医学材料等领域具有广阔的发展前景. 其中, 我们在光子晶体传感器、光电化学分解水、微透镜阵列等方面取得了一些独具特色的研究进展. 今后该领域值得关注的发展方向包括单层胶体晶体制备方法的改进[57,58]和结构的优化、模板复制方法的创新和材料体系的拓展、二维有序阵列的性能优化和新功能发掘.

参考文献

1 Lei Y, Yang S, Wu M, et al. Surface patterning using templates: Concept, properties and device applications. Chem Soc Rev, 2011, 40: 1247–1258

2 Warkiani M E, Bhagat A A S, Khoo B L, et al. Isoporous micro/nanoengineered membranes. ACS Nano, 2013, 7: 1882–1904

3 Yu N, Capasso F. Flat optics with designer metasurfaces. Nat Mater, 2014, 13: 139–150

4 Karg M, König T A F, Retsch M, et al. Colloidal self-assembly concepts for light management in photovoltaics. Mater Today, 2015, 18: 185–205

5 Cai J, Qi L. Recent advances in antireflective surfaces based on nanostructure arrays. Mater Horiz, 2015, 2: 37–53

6 Wang Z, Cao D, Xu R, et al. Realizing ordered arrays of nanostructures: A versatile platform for converting and storing energy efficiently. Nano Energy, 2016, 19: 328–362

7 Vogel N, Retsch M, Fustin C A, et al. Advances in colloidal assembly: The design of structure and hierarchy in two and three dimensions. Chem Rev, 2015, 115: 6265–6311

8 Phillips K R, England G T, Sunny S, et al. A colloidoscope of colloid-based porous materials and their uses. Chem Soc Rev, 2016, 45: 281–322

9 Ye X, Qi L. Two-dimensionally patterned nanostructures based on monolayer colloidal crystals: Controllable fabrication, assembly, and applications. Nano Today, 2011, 6: 608–634

10 Ye X, Qi L. Recent advances in fabrication of monolayer colloidal crystals and their inverse replicas. Sci Chin Chem, 2014, 57: 58–69

11 Li Y, Duan G, Liu G, et al. Physical processes-aided periodic micro/nanostructured arrays by colloidal template technique: Fabrication and applications. Chem Soc Rev, 2013, 42: 3614–3627

12 Geng C, Wei T, Wang X, et al. Enhancement of light output power from LEDs based on monolayer colloidal crystal. Small, 2014, 10: 1668–1686

13 Zhang Z, Geng C, Hao Z, et al. Recent advancement on micro-/nano-spherical lens photolithography based on monolayer colloidal crystals. Adv Colloid Interface Sci, 2016, 228: 105–122

14 Li Y, Qi L M. Advances in fabrication of two-dimensionally ordered porous membranes by nanosphere lithography at the gas-liquid interface (in Chinese). Acta Chim Sin, 2015, 73: 869–876 [李扬, 齐利民. 气液界面胶体球刻蚀法制备二维有序多孔薄膜. 化学学报, 2015, 73: 869–876]

15 Cai Z, Smith N L, Zhang J T, et al. Two-dimensional photonic crystal chemical and biomolecular sensors. Anal Chem, 2015, 87: 5013–5025

16 Ye X, Li Y, Dong J, et al. Facile synthesis of ZnS nanobowl arrays and their applications as 2D photonic crystal sensors. J Mater Chem C, 2013, 1: 6112–6119

17 Li L, Jiao X, Chen D, et al. Facile fabrication of ultrathin metal-organic framework-coated monolayer colloidal crystals for highly efficient vapor sensing. Chem Mater, 2015, 27: 7601–7609

18 Li L, Jiao X, Cheng D, et al. One-step asymmetric growth of continuous metal-organic framework thin films on two-dimensional colloidal crystal arrays: A facile approach toward multifunctional superstructures. Cryst Growth Des, 2016, 16: 2700–2707

19 Cai Z, Kwak D H, Punihaole D, et al. A photonic crystal protein hydrogel sensor for candida albicans. Angew Chem Int Ed, 2015, 54: 13036–13040

20 Men D, Zhou F, Hang L, et al. A functional hydrogel film attached with a 2D Au nanosphere array and its ultrahigh optical diffraction intensity as a visualized sensor. J Mater Chem C, 2016, 4: 2117–2122

21 Jones M R, Osberg K D, Macfarlane R J, et al. Templated techniques for the synthesis and assembly of plasmonic nanostructures. Chem Rev, 2011, 111: 3736–3827

22 Hong G, Li C, Qi L. Facile fabrication of two-dimensionally ordered macroporous silver thin films and their application in molecular

sensing. Adv Funct Mater, 2010, 20: 3774–3783
23 Im H, Bantz K C, Lee S H, et al. Self-assembled plasmonic nanoring cavity arrays for SERS and LSPR biosensing. Adv Mater, 2013, 25: 2678–2685
24 Yang S, Slotcavage D, Mai J D, et al. Combining the masking and scaffolding modalities of colloidal crystal templates: Plasmonic nanoparticle arrays with multiple periodicities. Chem Mater, 2014, 26: 6432–6438
25 Yang S, Hricko P J, Huang P H, et al. Superhydrophobic surface enhanced Raman scattering sensing using Janus particle arrays realized by site-specific electrochemical growth. J Mater Chem C, 2014, 2: 542–547
26 Liu G, Li X, Wang W, et al. Gold binary-structured arrays based on monolayer colloidal crystals and their optical properties. Small, 2014, 10: 2374–2381
27 Zheng J, Dai Z, Mei F, et al. Micro-nanosized nontraditional evaporated structures based on closely packed monolayer binary colloidal crystals and their fine structure enhanced properties. J Phys Chem C, 2014, 118: 20521−20528
28 Lee C, Carney R P, Hazari S, et al. 3D plasmonic nanobowl platform for the study of exosomes in solution. Nanoscale, 2015, 7: 9290–9297
29 Zhang H, Liu M, Zhou F, et al. Physical deposition improved SERS stability of morphology controlled periodic micro/nanostructured arrays based on colloidal templates. Small, 2015, 11: 844–853
30 Zhang H, Zhou F, Liu M, et al. Spherical nanoparticle arrays with tunable nanogaps and their hydrophobicity enhanced rapid SERS detection by localized concentration of droplet evaporation. Adv Mater Interfaces, 2015, 2: 1500031
31 Paria D, Roy K, Singh H J, et al. Ultrahigh field enhancement and photoresponse in atomically separated arrays of plasmonic dimers. Adv Mater, 2015, 27: 1751–1758
32 Li C, Hong G, Qi L. Nanosphere lithography at the gas/liquid interface: A general approach toward free-standing high-quality nanonets. Chem Mater, 2010, 22: 476–481
33 Li Y, Ye X, Ma Y, et al. Interfacial nanosphere lithography toward Ag_2S-Ag heterostructured nanobowl arrays with effective resistance switching and enhanced photoresponses. Small, 2015, 11: 1183–1188
34 Wang W, Dong J, Ye X, et al. Heterostructured TiO_2 nanorod@nanobowl arrays for efficient photoelectrochemical water splitting. Small, 2016, 12: 1469–1478
35 Wang X, Long R, Liu D, et al. Enhanced full-spectrum water splitting by confining plasmonic Au nanoparticles in N-doped TiO_2 bowl nanoarrays. Nano Energy, 2016, 24: 87–93
36 Ji L, McDaniel M D, Wang S, et al. A silicon-based photocathode for water reduction with an epitaxial $SrTiO_3$ protection layer and a nanostructured catalyst. Nat Nanotechnol, 2015, 10: 84–90
37 Zhu J, Hsu C M, Yu Z, et al. Nanodome solar cells with efficient light management and self-cleaning. Nano Lett, 2010, 10: 1979–1984
38 Yang S C, Yang D J, Kim J, et al. Hollow TiO_2 hemispheres obtained by colloidal templating for application in dye-sensitized solar cells. Adv Mater, 2008, 20: 1059–1064
39 Hörantner M T, Zhang W, Saliba M, et al. Templated microstructural growth of perovskite thin films via colloidal monolayer lithography. Energy Environ Sci, 2015, 8: 2041–2047
40 Meng K, Gao S, Wu L, et al. Two-dimensional organic-inorganic hybrid perovskite photonic films. Nano Lett, 2016, 16: 4166–4173
41 Zheng X, Wei Z, Chen H, et al. Designing nanobowl arrays of mesoporous TiO_2 as an alternative electron transporting layer for carbon cathode-based perovskite solar cells. Nanoscale, 2016, 8: 6393–6402
42 Aizenberg J, Tkachenko A, Weiner S, et al. Calcitic microlenses as part of the photoreceptor system in brittlestars. Nature, 2001, 412: 819–822
43 Li C, Qi L. Bioinspired fabrication of 3D ordered macroporous single crystals of calcite via a transient amorphous phase. Angew Chem Int Ed, 2008, 47: 2388–2393
44 Li C, Hong G, Yu H, et al. Facile fabrication of honeycomb-patterned thin films of amorphous calcium carbonate and mosaic calcite. Chem Mater, 2010, 22: 3206–3211
45 Ye X, Zhang F, Ma Y, et al. Brittlestar-inspired microlens arrays made of calcite single crystals. Small, 2015, 11: 1677–1682
46 Lan Y, Wang S, Yin X, et al. 2D-ordered dielectric sub-micron bowls on a metal surface: A useful hybrid plasmonic-photonic structure. Nanoscale, 2016, 8: 13454–13462
47 Sabri Y M, Kandjani A E, Ippolito S J, et al. Ordered monolayer gold nanourchin structures and their size induced control for high gas sensing performance. Sci Rep, 2016, 6: 24625
48 Hang L, Zhao Y, Zhang H, et al. Copper nanoparticle@graphene composite arrays and their enhanced catalytic performance. Acta Mater, 2016, 105: 59–67
49 Zhao Y, Hu L, Gao S, et al. One-step self-assembly fabrication of high quality $Ni_xMg_{1-x}O$ bowl-shaped array film and its enhanced photocurrent by Mg^{2+} doping. Adv Funct Mater, 2015, 25: 3256–3263

50 Gao T, Wang B, Ding B, et al. Uniform and ordered copper nanomeshes by microsphere lithography for transparent electrodes. Nano Lett, 2014, 14: 2105−2110
51 Shi X B, Qian M, Wang Z K, et al. Nano-honeycomb structured transparent electrode for enhanced light extraction from organic light-emitting diodes. Appl Phys Lett, 2015, 106: 223301
52 Dev A, Choudhury B D, Abedin A, et al. Fabrication of periodic nanostructure assemblies by interfacial energy driven colloidal lithography. Adv Funct Mater, 2014, 24: 4577–4583
53 Vogel N, Belisle R A, Hatton B, et al. Transparency and damage tolerance of patternable omniphobic lubricated surfaces based on inverse colloidal monolayers. Nat Commun, 2013, 4: 2176
54 Chang W Y, Wu Y, Chung Y C. Facile fabrication of ordered nanostructures from protruding nanoballs to recessional nanosuckers via solvent treatment on covered nanosphere assembled monolayers. Nano Lett, 2014, 14: 1546–1550
55 Hu C, Lan Y, West K R, et al. Cucurbit[8]uril-regulated nanopatterning of binary polymer brushes via colloidal templating. Adv Mater, 2015, 27: 7957–7962
56 Wang P Y, Bennetsen D T, Foss M, et al. Modulation of human mesenchymal stem cell behavior on ordered tantalum nanotopographies fabricated using colloidal lithography and glancing angle deposition. ACS Appl Mater Interfaces, 2015, 7: 4979–4989
57 Park C, Lee T, Xia Y, et al. Large-area assembly of a single-crystal monolayer of spherical particles by unidirectional rubbing. Adv Mater, 2014, 26: 4633–4638
58 Gao P, He J, Zhou S, et al. Large-area nanosphere self-assembly by a micro-propulsive injection method for high throughput periodic surface nanotexturing. Nano Lett, 2015, 15: 4591–4598

Summary for “基于单层胶体晶体的功能性二维有序阵列研究进展”

Progress in functional 2D ordered arrays based on monolayer colloidal crystals

LI Yang, WANG WenHui & QI LiMin*

Beijing National Laboratory for Molecular Sciences, College of Chemistry and Molecular Engineering, Peking University, Beijing 100871, China
* Corresponding author, E-mail: liminqi@pku.edu.cn

Two-dimensionally (2D) ordered micro- and nanostructure arrays have attracted considerable attention because of their novel and/or enhanced properties arising from the patterned structures. Monolayer colloidal crystals (MCCs) assembled from colloidal spheres have been widely employed for the controllable fabrication of a variety of 2D ordered micro- and nanostructure arrays because this strategy has been demonstrated to be facile, inexpensive, efficient, and versatile. This review paper summarizes the recent progress in the functional 2D ordered arrays based on MCCs, including their applications in 2D photonic crystal sensors, plasmonic nanostructure arrays, solar energy conversion devices, optic and optoelectronic devices, surface wetting and adhesion, biomedical materials, etc. Particular attention is paid to our recent advances in the controlled fabrication and applications of ZnS nanobowl arrays, heterostructured Ag_2S-Ag nanobowl arrays, heterostructured TiO_2 nanorod@nanobowl arrays, and single crystal calcite microlens arrays. Firstly, large-area ZnS nanobowl arrays with a monolayer inverse opal structure were synthesized facilely by nanosphere lithography at solution surface through direct solution deposition. Owing to the 2D periodic structure of the hexagonally ordered nanobowl arrays and the high refractive index of ZnS, the obtained ZnS nanobowl arrays showed intensive structural colors and tunable photonic band-gap properties. The as-prepared ZnS nanobowl arrays can be used as a sensitive 2D photonic crystal sensor for fast detection of organic solvents and for visual oil sensing. After surface functionalization, the ZnS nanobowl arrays can be used as an effective 2D photonic crystal biosensor for sensitive detection of avidin molecules. Secondly, unique Ag_2S-Ag heterostructured nanobowl arrays consisting of Ag_2S nanonets lying on Ag nanobowl arrays were fabricated by two-step nanosphere lithography at the gas-liquid interface. The heterostructured nanobowl arrays exhibited effective resistance switching behaviors, thus showing the potential application in electronic switches and memory devices. Meanwhile, the heterostructured nanobowl arrays exhibited enhanced photocatalytic activity owing to their unique structure when they were used as a photoanode for photoelectrochemical (PEC) water splitting. This result may open up new possibilities for facile and rational synthesis of large-area ordered arrays of semiconductor-noble metal hybrid nanostructures with multifunctions. Thirdly, heterostructured TiO_2 nanorod@nanobowl (NR@NB) arrays consisting of rutile TiO_2 nanorods grown on the inner surface of arrayed anatase TiO_2 nanobowls were designed and fabricated as a new type of photoanodes for PEC water splitting. The unique heterostructures with a hierarchical architecture were readily fabricated by interfacial nanosphere lithography followed by hydrothermal growth. The heterostructured TiO_2 NR@NB arrays on the FTO substrate showed significantly enhanced PEC properties for water splitting because they possessed multiple scattering centers, increased electrolyte accessible surface area, and beneficial anatase-rutile heterojunction. This work may open new avenues towards building complex semiconductor nanostructures with desirable architectures for efficient harvesting and utilization of solar energy. Lastly, unprecedented concave microlens arrays (MLAs) made of calcite single crystals with tunable crystal orientations were readily fabricated by MCC-assisted epitaxial growth in solution without additives under ambient conditions. Calcite single crystal MLAs with two different crystallographic orientations, namely, calcite (104) microlens arrays and calcite (001) microlens arrays, were produced using selected calcite substrates, respectively. While the non-birefringent calcite (001) microlens array showed excellent imaging performance like brittlestar’s microlens arrays, the birefringent calcite (104) microlens array exhibited remarkable polarization-dependent optical properties. In general, this work may open new pathways towards the fabrication of micropatterned single crystals for various optical applications and shed light on fundamental mechanisms in biomineralization. After a brief summary of the recent progress in this research field, the challenges and perspectives for future research are addressed.

monolayer colloidal crystal, nanosphere lithography, 2D ordered array, nanostructure, microstructure

doi: 10.1360/N972016-00824